IET Communications

Research Article

IET Journals
The Institution of Engineering and Technology

Optimisation-based deployment of beacons for indoor positioning using wireless communications and signal power ranking

ISSN 1751-8628
Received on 27th March 2019
Revised 3rd March 2020
Accepted on 30th June 2020
E-First on 12th October 2020
doi: 10.1049/iet-com.2019.0201
www.ietdl.org

Ching-Lung Chang[1,2], *Chuan-Yu Chang*[1,2], *Shuo-Tsung Chen*[1] ✉, *Jhe-Ming Syu*[1]

[1]*Department of Computer Science and Information Engineering, National Yunlin University of Science and Technology, Yunlin 64002, Taiwan*
[2]*Intelligence Recognition Industry Service Research Center (IR-IS Research Center), National Yunlin University of Science and Technology, Yunlin 64002, Taiwan*
✉ *E-mail: shough34@yahoo.com.tw*

Abstract: Beacon-based indoor positioning is popular in recent years. In this work, the authors aim to enhance the positioning accuracy by proposing signal power ranking (SPR) and solving related optimisation-based deployment problem of beacons using wireless communication and Bluetooth 4.0 Bluetooth low-energy network technologies. The authors first adopt grid-based field to be the proposed deployment field. Second, they convert the received signal strength indicator (RSSI) to several levels called SPR. Third, an optimisation-based model for deployment problem of beacons in indoor positioning is proposed on the basis of the above two considerations. The proposed model is to minimise the number of beacons required under some fundamental conditions including full coverage and full discrimination, respectively. Finally, the algorithm of simulated annealing is applied to solve the linear programming problem in this model. By the optimal results, the user can obtain a vector table of RSSI for each location efficiently in the test field. On the other hand, the user in the test field can receive the beacon RSSI value at the same time. In order to determine the user's location, the received beacon RSSI value is compared with the values in the vector table.

1 Introduction

Positioning can be divided into outdoor positioning and indoor positioning. Outdoor positioning mainly uses Global Positioning Systems (GPS) and other methods to achieve the purpose of positioning. In the near future, indoor positioning will gain more demand as people spend >70% of their lives in the indoor environment. However, satellite signals in GPS technology cannot penetrate in the indoor environment since they are blocked by building obstructions thus satellite signal cannot provide good accuracy in indoor environments [1–3]. Indoor positioning has been a very important topic because it needs to locate and guide people to some place. Therefore, precise indoor positioning systems with low cost and scalability are required [4–6].

In [7], estimated distances are applied to compute the most probable coordinates by triangle geometry. With Bluetooth low-energy (BLE), the distance to a beacon is measured by reading received signal strength indicator (RSSI) which is mapped into actual distance according to radiofrequency propagation model [8]. In [9, 10], the RSSI-to-distance mapping model is regarded as unstable due to the unreliable distance estimation in BLE. Chen *et al.* [11, 12] combined the pedestrian dead reckoning with a weighted pass loss algorithm that is based on the log-distance path loss model. Zhuang *et al.* [13] proposed an algorithm that uses the combination of the channel-separate polynomial regression model, channel-separate fingerprinting, outlier detection and extended Kalman filtering for smartphone-based indoor localisation with BLE beacons. The proposed algorithm achieved the accuracy of <2.56 m at 90% of the time with dense deployment of BLE beacons thus useful to improve the localisation accuracy in environments with sparse beacon deployment. In [14], the authors discussed an indoor-positioning method of weighted centroid localisation (WCL) using RSSI observed from neighbouring BLE beacons. The WCL is evaluated in their testbed building and analysed to configure its parameters for indoor positioning. Danis and Cemgil [15] introduced a high precision localisation and tracking method that makes use of cheap BLE beacons only to track the position of a moving sensor by integrating highly unreliable and noisy BLE observations streaming from multiple locations. A novel aspect of their approach is the development of an observation model, specifically tailored for RSSI fingerprints. In [16], authors used the similarities between received signal strength (RSS) sequence and the reference fingerprints without training are computed and embedded into a particle filter to track the positions of users in wireless indoor environments.

In this work, we proposed an optimisation-based model for the deployment of beacons in indoor positioning. Accordingly, a linear programming problem is generated and the algorithm of simulated annealing (SA) is applied to solve the problem successfully. The detailed procedure is introduced as follows. First, we adopt the grid-based field to be our testing field for the deployment of beacons. The testing field is divided into $n \times n$ grids of the same size. Then, for each kind of beacon's power, we convert the RSSI to several levels called signal power ranking (SPR). In order to have the lowest cost and the best deployment, we design an optimisation-based model as a linear programming model satisfying two fundamental demands, complete covered and complete identification. Finally, the algorithm of SA is applied to solve the linear programming problem derived from the model and thus have the optimal deployment for beacons. By the optimal deployment, the user can obtain a vector table of RSSI for each location with the best effectiveness in the test field. On the other hand, the user in the test field can receive the beacon RSSI value at the same time. In order to determine the user's location, the received beacon RSSI value is compared with the values in the vector table.

The rest of this paper is organised as follows. Section 2 reviews background and related work. Section 3 presents the proposed system with optimisation-based model and its solving approach. Section 4 shows the experimental environment and results. Section 5 concludes our work.

2 Backgrounds and preliminary

This section first reviews some backgrounds including indoor positioning, Bluetooth 4.0 and beacon. Next, preliminary such as the algorithm of SA is prepared.

Table 1 Comparison of wireless sensing technology

	RFID	Zigbee	Wi-Fi	Bluetooth
transmission speed	106 kpbs	205 kbps	300 Mbps	1 Mbps
transmission distance, m	1.2	50–300	100–300	1–50
consumption	0(mA)	5	10–50	<15
cost	middle	middle	high	low
advantage	wide applicability	low power consumption, low cost	high speed, popularity	low consumption, cost, and integrated
application	daily common	industrial and engineering applications	the application of wireless internet access	easy to integrate applications in mobile devices

Table 2 Comparison of each version for Bluetooth

Mainstream specifications				
Version	2.0 + EDR	2.1 + EDR	3.0 + HS	4.0
published	2004.11	2007.7	2009.4	2010.6
speed	1–3 Mbps	1–3 Mbps	24 Mbps	normal: 3M bps HS: 24 Mbps
specifications	enhanced data transfer rate	simple security pairing	AMP technology, enhanced power control	low power consumption, low cost

Table 3 Comparison of classic Bluetooth with low power consumption

	Classic	Low power
Frequency	2.4 GHZ	2.4 GHZ
transmission rate	1–3 Mbps	1 Mbps
effective distance	10	60
Consumption	30	<15
sleep mode	no	yes

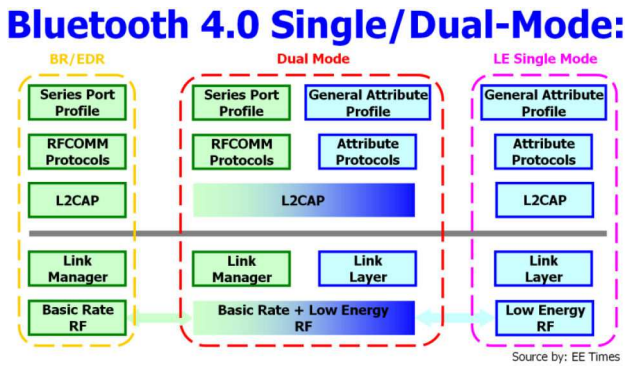

Fig. 1 *Bluetooth 4.0 single/dual-mode beacon*

2.1 Indoor positioning

With the widespread advances of devices and technologies, indoor real-time positioning (simply indoor positioning) has been gaining relevance. It tracks objects, vehicles or people within a building or enclosed infrastructure. Current indoor positioning technology can be divided into radio frequency identification (RFID), Wi-Fi, Bluetooth, Zigbee, Computer Vision, Ultrasound, Infrared Ray and so on [10–26]. Wireless sensing technologies such as RFID, Wi-Fi, Bluetooth, Zigbee are more popular. Their specification and performance comparisons are shown in Table 1.

2.2 Bluetooth 4.0

Bluetooth is a wireless technology standard for exchanging data over short distances from fixed and mobile devices and building personal area networks. The most important feature of Bluetooth 4.0 is the power saving technology which is known as BLE, very low execution and standby power consumption, which allows a button battery to work continuously for several years, in addition to low cost and cross-operational features, >100-m long and long-distance communication and many other features [27]. It can be used for a pedometer, heart rate monitor, intelligent instrumentation, sensing network, internet of things and many other areas [28].

Bluetooth 4.0 is still backwards compatible (as shown in Table 2), including the Bluetooth technology specification (Bluetooth 2.1 + EDR) and the maximum speed of 24 Mbps Bluetooth high-speed technology (Bluetooth 3.0 + HS) specification, three kinds of technical specifications not only can be used alone but also run at the same time.

The low power Bluetooth technology as the core framework can make the equipment not work in a dormant state, wake up when you need to use the Bluetooth function. It can effectively reduce the power consumption and effectively prolong the service life of the battery of Bluetooth devices. In the transmission distance, the effective transmission distance is effectively improved, and the radio frequency range is adjusted according to different applications. Traditional Bluetooth and low-power Bluetooth are shown below, as shown in Table 3.

Now the latest smartphones have been applied to the Bluetooth 4.0 technology. Bluetooth 4.0 supports two subordinate modes: dual-mode and single-mode, as shown in Fig. 1. It can support both basic technology and Bluetooth low-power device called dual-mode (dual-mode) device: basically, mobile phone and desktop computer Bluetooth system are dual-mode devices, if only support Bluetooth low-power devices known as single-mode devices, single-mode devices are generally used in devices with battery life considerations.

Beacon's main hardware architecture is Bluetooth 4.0 hardware, which takes advantage of BLE, long launch distance and low cost of the chip. So as long as the current Apple Corp ios7 and hardware collocation Bluetooth 4 chip products can support beacon technology and Android system as long as the 4.3 version of the above can support [29].

A basic beacon indoor positioning system [28] can be divided into three parts including support for Bluetooth 4.0 intelligent mobile devices, beacon Bluetooth launchers and related applications APP software. When the mobile device enters the beacon signal range, the APP will be able to send the wireless signal from the beacon received via Bluetooth if the mobile device has turned on the Bluetooth function and the download is related to the APP, and from the received signal to determine the beacon signal strength and device identification code. Use of this APP information can be calculated with the beacon transmitter relative distance, but also by this distance to complete the reservation or push message.

As shown in Fig. 2, beacon packets can be divided into five parts:

(i) *Beacon Prefix (9 bytes)*: This is a fixed value, APP through this value is used to identify whether the device is iBeacon Node.
(ii) *Proximity UUID (16 bytes)*: Used to distinguish with other uses of beacon, assuming a shopping mall has multiple beacons, have a common UUID, so by different UUID can distinguish between those who do not belong to this application scene
(iii) *Major (2 bytes)*: Like grouping of group ID, UUID assume the same mall, but the mall different types of stores, do have different major distinction.
(iv) *Minor (2 bytes)*: Is the number of this beacon, so Major + Minor + Proximity UUID makes it a unique beacon.
(v) *Tx Power (1 byte)*: The delegate is the RSSI that beacon has received, and it is possible to estimate the current position with this beacon distance.

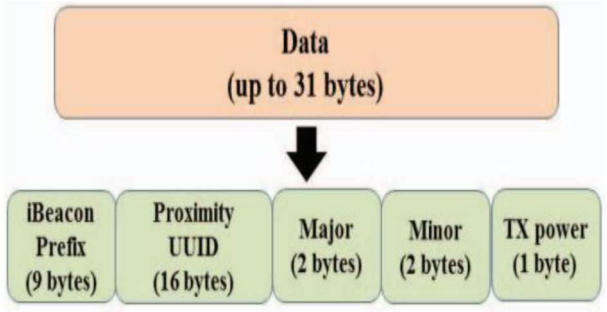

Fig. 2 *Beacon data*

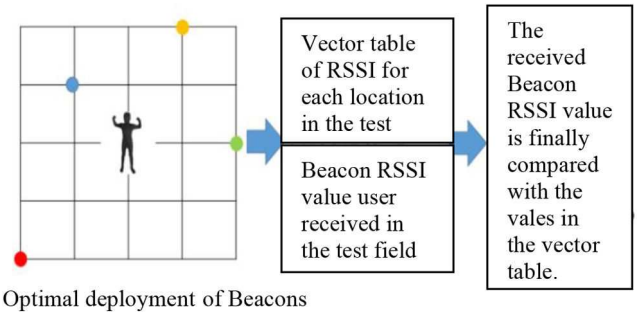

Fig. 3 *Flowchart of determining the user's location with the proposed optimal deployment of beacons*

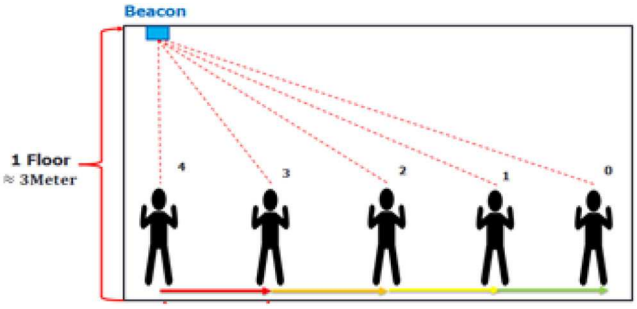

Fig. 4 *Beacons are deployed on the ceiling to reduce the interferences and the RSSI values received are measured from the horizontal distance just below the beacon*

3 Proposed system with optimisation-based model and its solving approach

This section presents the proposed system with optimisation-based model and its solving approach. As shown in Fig. 3, the outline of the proposed system architecture is as follows. First of all, we deploy beacons using Bluetooth 4.0 BLE on the ceiling to reduce the interferences and measure the RSSI value received from the horizontal distance just below the beacon. For the deploying, we proposed an optimisation-based model and the corresponding optimisation solver. Next, user can obtain a vector table of RSSI for each location in the test field, respectively. On the other hand, user in the test field can receive the beacon RSSI value at the same time. In order to determine user's location, the received beacon RSSI value is finally compared with the vales in the vector table such as the last step in Fig. 3. The detail of the proposed system architecture is introduced in Sections 3.1–3.4.

3.1 Distance judgement corresponds to signal strength

For positioning, Bluetooth 4.0BLE technology in beacon generally adopts RSSI to present signal strength and thus judge distance. However, the signal strength is easily susceptible to interference from the environment or obstacles and is not very stable so that the judging accuracy of RSSI is low. To improve this drawback, we proposed several methods as follows. First of all, we deploy beacons on the ceiling to reduce the interferences and measure the RSSI value received from the horizontal distance just below the beacon, as shown in Fig. 4.

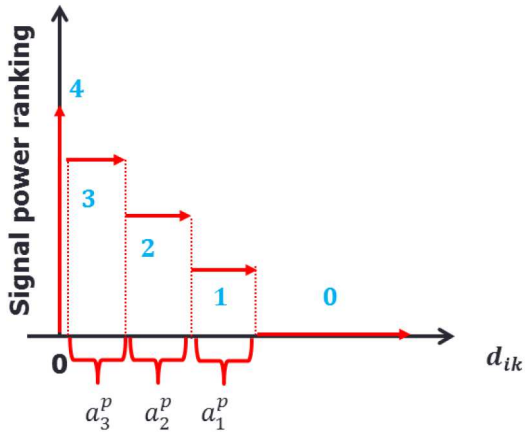

Fig. 5 *RSSI SPR*

Next, the testing field is cut into $n \times n$ grids of the same size so that the Bluetooth transmitters named beacon are deployed in the grid and then the following steps are proposed to enhance the judging accuracy:

(i) Signal strength p_d according to distance can be represented by (1) (a path-loss model), in which n is a signal attenuation constant, d is the distance between transmitter and receiver and p_0 is the strength of the transmission signal measured at a distance of one metre from the transmitter

$$p_d = p_0 - 10n\log_{10}(d) \tag{1}$$

Convert the RSSI to a different level called the SPR by using the concept of the step function to have the following distance relationships. As shown in Fig. 5, SPR can be expressed as

$$\text{SPR} = \sum_{r=r_1}^{r_p} rf(d_{ij}) \tag{2}$$

where d_{ij} denotes the distance between ith positioned grid and the beacon deployed in jth grid; r denotes the signal strength level when the transmission power is p and $f(\bullet)$ is an indication function defined as

$$f(d_{ij}) = \begin{cases} 1, & \text{if } d_{ij} \subseteq a_{r_p}^p \\ 0, & \text{otherwise} \end{cases}$$

where $a_{r_p}^p$ denotes the distance under level r_p when the transmission power is p, that is if the distance d_{ij} between positioned grid i and the beacon deployed in grid j is inside $a_{r_p}^p$, then SPR is r_p. Different level of signal strength can reduce the positioning errors of RSSI caused by the interferences.

(ii) Show the positioned grids by using ranking vector (RV) defined as

$$\boldsymbol{V}_i = (v_{i1}, v_{i2}, \ldots, v_{ij}, \ldots) \tag{3}$$

where $\boldsymbol{V}_i$ is the RV of the positioned grid i and v_{ij} is the SPR of the positioned grid i receiving the signal of beacon deployed in grid j. In the beacon deploying process, the power distance of any two grid levels should be made as large as possible to increase the accuracy of positioning.

3.2 Proposed optimisation-based models

Without loss of generality, as shown in Fig. 6, beacons are arranged in the centre of the grid and each beacon has its coverage. For example, the coverage of the fifth beacon in the figure is the red

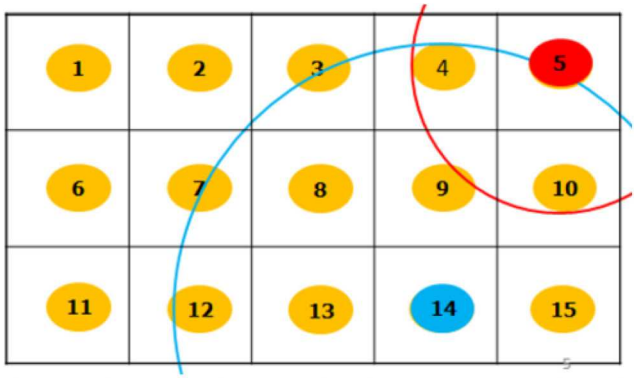

Fig. 6 *Placement diagram for beacons arranged in the centre of the grid and each beacon has its coverage*

Table 4 Model's objective

Target	Results	How to reach
full coverage	each grid location is overwritten	all locations in the field are covered
full discrimination	each grid location can be identified	each grid power vector is different
min cost	less sensor number	with a smaller number to achieve the goal

circle, and the coverage of the 14th beacon is the blue circle. In order to have the lowest cost and the best deployment, we consider optimising the beacon numbers and the positioning accuracy under two fundamental demands, complete covered and complete identification. In other words, the proposed optimisation-based models should match three targets listed in Table 4.

The given parameters and unknown decision variables with respect to the proposed optimisation-based models are first listed in the following.

Parameters

I, the number of positioned grids.

$J, J \le I$, the number of possible grids of beacon deployed.

P, kind of transmission power of beacon.

$R_{\mathrm{p}} = \{r_1, r_2, \cdots, r_{\mathrm{p}}\}, p \in P$, signal strength level corresponding to the transmission power p.

$A_{\mathrm{p}} = \{a_1^{\mathrm{p}}, a_2^{\mathrm{p}}, \cdots, a_{r_{\mathrm{p}}}^{\mathrm{p}}\}, r_{\mathrm{p}} \in R_{\mathrm{p}}$, distance range corresponding to level r_{p} with transmission power p.

$d_{ij}, i \in I, j \in J$, the distance between the positioned grid I and beacon j.

$f(d_{ij})$, the indication function mentioned in Section 3.1.

Unknown decision variables

$x_i^{\mathrm{p}}, i \in I, p \in P$, $x_i^{\mathrm{p}} = 1$ when the beacon is deployed to grid i and the transmit power is p; otherwise $x_i^{\mathrm{p}} = 0$

$\boldsymbol{V}_i = (v_{i1}, v_{i2}, \ldots, v_{ij}, \ldots, v_{iJ})$, V_i is the RV of the positioned grid i and v_{ij} is the SPR of the positioned grid i receiving the strength of Beacon deployed in grid j.

Second, we introduce the constraints according to the real conditions in positioning as follows:

Constraints

$\sum_{p \in P} x_i^{\mathrm{p}} \le 1, \ \forall i \in I$, $x_i^{\mathrm{p}} = 1$ when beacon is deployed to grid i and the transmit power is p; otherwise $x_i^{\mathrm{p}} = 0$ (or $x_i^{\mathrm{p}} \in \{0,1\}, \ \forall i \in I, \forall p \in P$)

$v_{ij} = \sum_{p \in P} x_i^{\mathrm{p}} \left\{ \sum_{r=1}^{r_{\mathrm{p}}} r f(d_{ij}) \right\}$, SPR of the positioned grid i received from the beacon deployed in the grid k when $i \neq k$ $\forall i \in I, \forall j \in J$

$v_{ij} = \sum_{p \in P} x_i^{\mathrm{p}} r_{\mathrm{p}}, \ \forall i \in I, j = i$, SPR of the positioned grid i received from the beacon deployed in the grid k when $i = k$.

$\sum_{j=1}^{J} v_{ij} \ge 1, \ \forall i \in I$, ensure the grid i to receive an SPR for full coverage of the testing field

$\sum_{j=1}^{J} (v_{lj} - v_{kj}) \ge \Phi, \ \forall l, k \in I$, power distance $\sum_{j=1}^{J} (v_{lj} - v_{kj}), \ \forall l, k \in I$ between two positioned grids in the testing field should be greater than a positive number Φ

$m - \sum_{i \in I} \sum_{p \in P} x_i^{\mathrm{p}} = \Psi$, the number of grids that are not deployed $m - \sum_{i \in I} \sum_{p \in P} x_i^{\mathrm{p}}$ is equal to a natural number Ψ or zero

Based on the above consideration, we propose two optimisation-based models, optimisation-based model phase I and optimisation-based model phase II. By introducing a weighting parameter α, the optimisation-based mode phase I is listed as follows:

Optimisation-based model phase I

$$\text{maxmize} \ \ \alpha\Phi + (1-\alpha)\Psi$$

subject to

$$\text{(i)} \ \sum_{p \in P} x_i^{\mathrm{p}} \le 1, \ \forall i \in I$$

$$\text{(ii)} \ v_{ij} = \sum_{p \in P} x_i^{\mathrm{p}} \left\{ \sum_{r=1}^{r_{\mathrm{p}}} r f(d_{ij}) \right\}, \ \forall i \in I, \forall j \in J$$

$$\text{(iii)} \ v_{ij} = \sum_{p \in P} x_i^{\mathrm{p}} r_{\mathrm{p}}, \ \forall i \in I, j = i$$

$$\text{(iv)} \ \sum_{j=1}^{J} v_{ij} \ge 1, \ \forall i \in I$$

$$\text{(v)} \ \sum_{j=1}^{J} (v_{lj} - v_{kj}) \ge \Phi, \ \forall l, k \in I$$

$$\text{(vi)} \ m - \sum_{i \in I} \sum_{p \in P} x_i^{\mathrm{p}} = \Psi$$

The previous model applies the weight α to balance the power distance and the number of grids that are not deployed. However, sometimes users consider to maximise the power distance under the bounded number of positioned grids. Thus, the optimisation-based mode phase I is rewritten as the optimisation-based mode phase II.

Optimisation-based model phase II

$$\text{maxmize} \ \ \Phi$$

subject to

$$\text{(i)} \ \sum_{p \in P} x_i^{\mathrm{p}} \le 1, \ \forall i \in I$$

$$\text{(ii)} \ v_{ij} = \sum_{p \in P} x_i^{\mathrm{p}} \left\{ \sum_{r=1}^{r_{\mathrm{p}}} r f(d_{ij}) \right\}, \ \forall i \in I, \forall j \in J$$

$$\text{(iii)} \ v_{ij} = \sum_{p \in P} x_i^{\mathrm{p}} r_{\mathrm{p}}, \ \forall i \in I, j = i$$

$$\text{(iv)} \ \sum_{j=1}^{J} v_{ij} \ge 1, \ \forall i \in I$$

$$\text{(v)} \ \sum_{i \in I} \sum_{p \in P} x_i^{\mathrm{p}} \le \Psi$$

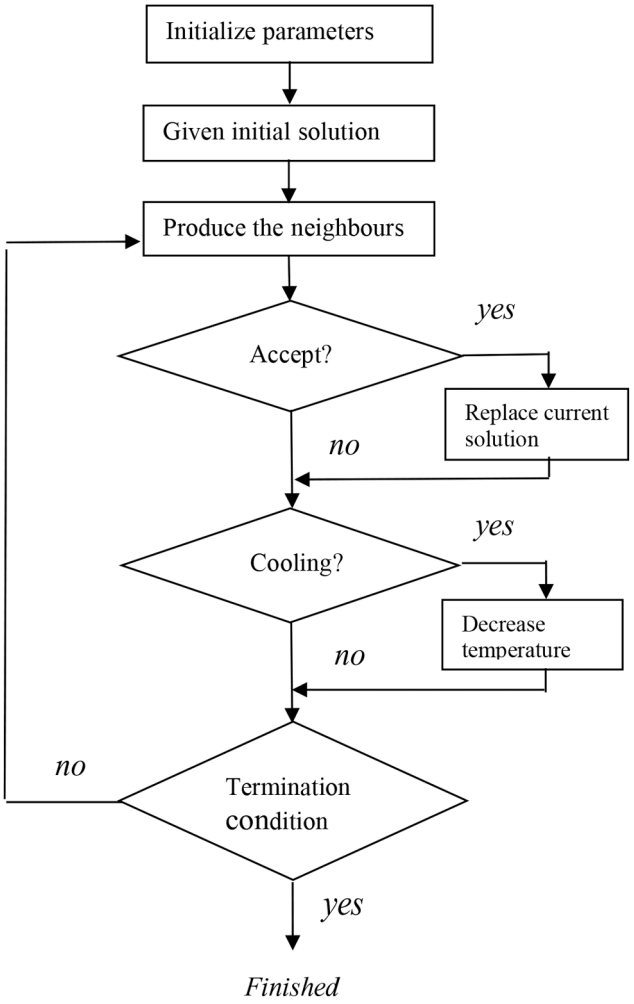

Fig. 7 *Flowchart of solving the proposed optimisation model using SA*

3.3 Optimal solution

SA is a probabilistic technique for approximating the global optimum of a given function. Specifically, it is metaheuristic to approximate global optimisation in a large search space. It is often used when the search space is discrete. In general, the SA algorithms work as follows. At each time step, the algorithm randomly selects a solution close to the current one, measures its quality and then decides to move to it or to stay with the current solution based on either one of two probabilities between which it chooses on the basis of the fact that the new solution is better or worse than the current one. During the search, the temperature is progressively decreased from an initial positive value to zero and affects the two probabilities: at each step, the probability of moving to a better new solution is either kept to 1 or is changed towards a positive value; instead, the probability of moving to a worse new solution is progressively changed towards zero [30].

The following pseudocode presents the SA heuristic as described above. It starts from a state s_0 and continues until a maximum of $k_{\max}$ steps have been taken. In the process, the call neighbour(s) should generate a randomly chosen neighbour of a given state s; the call random (0, 1) should pick and return a value in the range [0, 1], uniformly at random. The annealing schedule is defined by a temperature T. The algorithm of SA starts initially with T set to a high value (or infinity), and then it is decreased at each step following some annealing schedule, which may be specified by the user, but must end with $T = 0$ towards the end of the allotted time budget.

Let $s = s_0$.
For $k = 0$ through $k_{\max}$ (exclusive):
$T \leftarrow$ temperature($k/k_{\max}$)
Pick a random neighbour, $s_{\text{new}} \leftarrow$ neighbour(s)
If $P(E(s), E(s_{\text{new}}), T) \geq$ random(0, 1):
$s \leftarrow s_{\text{new}}$
Output: the final state s

The algorithm of SA is easy to be implemented by its simple concept and calculation. Due to the fact that the algorithm of SA is easy to be implemented by its simple concept and calculation, especially for beacon's embedded system, we adopt SA mentioned in Section 2.6 to find the optimal solution of the proposed model. As shown in Fig. 7, the detailed procedure of SA in solving the proposed model is introduced in the following steps.

Step 1. Setting the initialisation for parameters including initial temperature, final temperature, cooling rate and the number of iteration for a fixed temperature.

Step 2. Given the initial solution.

Step 3. Optimisation of a solution involves evaluating the neighbours of a state of the problem. We change the parameters to produce the neighbours by three methods:

(i) Deploy each beacon with power to a grid which is selected randomly. If there is already a deployment of beacon in some grid, move the beacon to another grid randomly.
(ii) Randomly selected a grid to change the beacon's power if the grid has a beacon.
(iii) Both (i) and (ii).

Step 4. The probability of making the transition from the current model state to a candidate new model state is specified by an acceptance probability function *P(E,E′,T)*, that depends on the energies E and E', and on a global time-varying parameter T called the temperature

$$P(E, E', T) = \begin{cases} 1, & \text{if } \Delta E \leq 0 \\ \mathrm{e}^{\left(\frac{-\Delta E}{T}\right)}, & \text{if } \Delta E > 0 \end{cases}$$

where $\Delta E = E' - E$. In case $\Delta E \leq 0$, the probability function $P(E, E', T)$ is equal to 1 indicating that the current model state of solution s is replaced by the candidate new model state of a neighbour solution s'. In case $\Delta E > 0$, the current model state of solution s is replaced by the candidate new model state of the neighbour solution s' when probability function $P(E, E', T) = \mathrm{e}^{((-\Delta E/T))}$ is greater than a threshold $H \in (0, 1)$. When this step is finished, the number of iterations plus one and go to step 5.

Step 5. When step 4 is finished, the number of iterations plus one and the temperature T is decreased by a cooling rate α to a new temperature $T' = \alpha T$.

Step 6. Check if the temperature reaches the final temperature to stop SA.

4. Experimental environment and results

This section shows the experimental environment, parameter setting, pre-processing and experimental results.

4.1 Experimental tools

This subsection introduces the hardware devices and software used in the experimental test and research of this paper. First, we show the hardware facilities including the smart mobile device ASUS Zenfone2 Laser and Bluetooth transmitter HEREBEACON. The specification of HEREBEACON is listed in Table 5.

Second, SA and Lingo 9.0 are both applied to the program in solving the proposed optimisation problem. To display the information received from HEREBEACON, we apply Eclipse 4.5 and Android SDK to build some functions in the smart mobile device ASUS Zenfone2 Laser.

Table 5 Specification of HEREBEACON

MCU	TI CC2541
Size	58 × 58 × 15, mm
Material	ABS
Protocol	Bluetooth® 4.0 with iBeacon certification
Security	support password for connection
radius power	0 to −23 dbm
transmission range	30 m, applicable for signal coverage optimisation
broadcasting interval	20–10,000 ms, applicable for signal coverage optimisation
sleep mode power consumption	5 μW
sleep mode power current	1 μA
supply voltage	3.0 V
Battery	AA*2
battery life	2.5 y

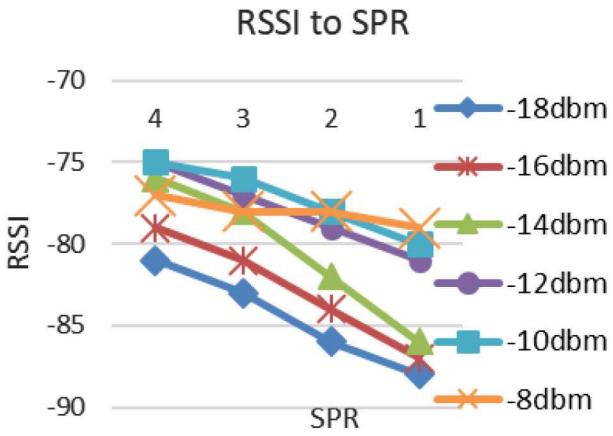

Fig. 8 *Relationship between signal strength RSSI and SPR*

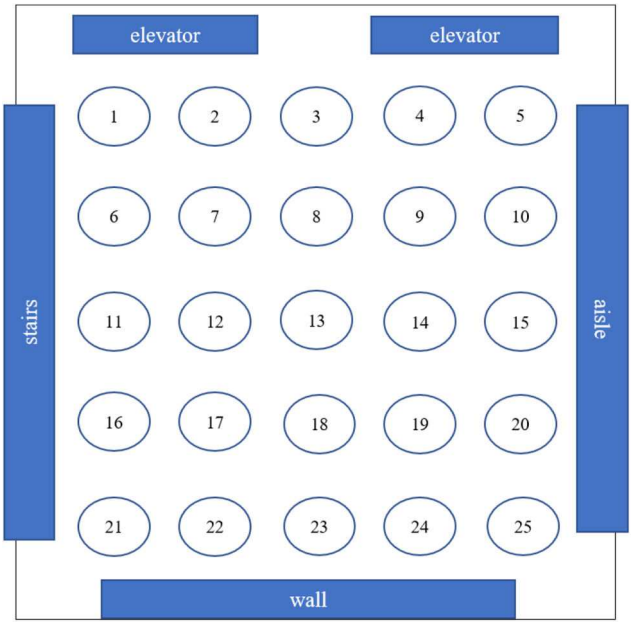

Fig. 9 *Experimental field with 5 m × 5 m grids, each side of the grid is 1 m*

4.2 Parameter setting and Pre-process

For experiments later, we need to first set the parameters including initial temperature, final temperature, cooling rate and the number of iteration. They are listed as follows:

Initial temperature: 10,000.
Final temperature: 1000.
Cooling rate: 0.9999.
Number of iteration for a fixed temperature: 1000.

Next, we need to have a pre-processing in testing the distances RSSI. Generally, high signal strength will result in almost no distinction among different distances while low signal strength will result in no signal received by users. In other words, the signal strength will affect the value received at different distances. Accordingly, we test the distances RSSI of each power to see which power can easily distinguish the level. As shown in Fig. 8, by testing 100 records for each power and distance we finally adopt −14 and −18 dBm, respectively. The relationship between signal strength and SPR is also shown in Fig. 8. In addition, we use the median filter to improve the value of the fluttering situation since the intensity of the signal in the environment is fluttering.

4.3 Experimental results

We will test the experimental fields of different sizes to verify our method. Fig. 9 shows the first experimental field which is surrounded by two elevators, stairs, one wall and one aisle. The ceiling height is 2.4 m. We plan the experimental field to be a square lattice with a side length of 1 to form the corresponding grid points, such as 5 m × 5 m field in Fig. 9.

The experimental results of the first experimental field are discussed separately according to the two optimisation models proposed.

4.3.1 Optimisation-based model phase I: Before testing lager fields, we first use two small fields of size 3 m × 2 m and 4 m × 3 m to verify whether SA works correctly. We adopt Lingo to do the verification where the weight α is from 0.1 to 0.5 to produce a different way to do the comparison. From the OBJ comparison in the field of size 3 m × 2 m shown in Table 6, one can observe that there is no difference between Lingo and SA even SA deploys two more points with $\alpha = 0.5$. From the OBJ comparison in the field of size 4 m × 3 m shown in Table 7, one can observe that there is only a little difference between Lingo and SA in $\alpha = 0.5$ and $\alpha = 0.5$. Due to the fact that the execution speed of LINGO in the field larger than 4 m × 3 m is obviously slower, Tables 8–10 list the

Table 6 Optimal results comparison between Lingo and SA in field 3 m × 2 m

α	Solver	ϕ	ψ	OBJ	(Grid, p)
0.1	Lingo	2	4	3.8	(4,1), (6,1)
	SA	2	4	3.8	(4,1), (6,1)
0.2	Lingo	2	4	3.6	(4,1), (6,1)
	SA	2	4	3.6	(4,1), (6,1)
0.3	Lingo	2	4	3.4	(4,1), (6,1)
	SA	2	4	3.4	(4,1), (6,1)
0.4	Lingo	2	4	3.2	(4,1), (6,1)
	SA	2	4	3.2	(4,1), (6,1)
0.5	Lingo	4	2	3	(1,1), (3,1), (4,1), (6,1)
	SA	2	4	3	(4,1), (6,1)

Table 7 Optimal results comparison between Lingo and SA in field 4 m × 3 m

α	Solver	ϕ	ψ	OBJ	(Grid, p)
0.1	Lingo	2	8	7.4	(4,2), (5,2), (8,2), (12,2)
	SA	2	9	8.3	(4,1), (8,2), (12,2)
0.2	Lingo	2	9	7.6	(5,2), (8,2), (10,1)
	SA	2	9	7.6	(5,2), (8,2), (10,1)
0.3	Lingo	2	9	6.9	(1,2), (5,2), (9,2)
	SA	2	9	6.9	(1,2), (5,2), (9,2)
0.4	Lingo	4	8	6.4	(3,1), (5,2), (7,1), (11,1)
	SA	4	8	6.4	(3,1), (5,2), (7,1), (11,1)
0.5	Lingo	10	3	6.5	(3,1), (5,2), (7,1), (11,1)
	SA	2	6	4.0	(3,1), (5,2), (7,1), (11,1)

Table 8 Optimal results using SA in field 5 m × 4 m

α	ϕ	ψ	OBJ	(Grid, p)
0.1	1	17	15.4	(2,1), (6,2), 10,2)
0.2	1	17	13.8	(3,2), (10,2), (13,2)
0.3	1	17	12.2	(3,2), (12,2), (18,2)
0.4	1	17	0.4	(4,2), (7,1), (9,2)

Table 9 Optimal results using SA in field 5 m × 5 m

α	ϕ	ψ	OBJ	(Grid, p)
0.1	3	18	16.5	(1,2), (3,2), (5,2), (19,2), (21,2), (23,2), (25,2)
0.2	3	18	15	(1,2), (3,2), (5,2), (19,2), (21,2), (23,2), (25,2)
0.3	3	18	13.5	(1,2), (3,2), (5,2), (19,2), (21,2), (23,2), (25,2)
0.4	7	16	12.4	(9,1), (10,1), (11,2), (13,1), (14,1), (15,1), (16,2), (17,2)
0.5	2	20	11	(6,2), (8,2), (12,2), (15,2), (19,2)

Table 10 Optimal results using SA in field 6 m × 6 m

α	ϕ	ψ	OBJ	(Grid, p)
0.1	3	24	21.9	(13,2), (14,1), (15,1), (16,1), (17,2), (18,2), (19,2), (20,1), (21,2), (22,2), (23,2), (24,1)
0.2	3	24	19.8	(13,2), (14,2), (15,2), (16,2), (17,2), (18,2), (19,2), (20,1), (21,2), (22,2), (23,1), (24,1)
0.3	8	22	17.8	(10,2), (13,1), (14,1), (15,1), (16,1), (17,1), (18,1), (19,1), (20,1), (21,1), (22,1), (23,1), (24,1), (26,1)
0.4	9	20	15.6	(2,2), (9,1), (13,2), (14,1), (15,1), (16,1), (17,1), (18,1), (19,1), (20,1), (21,1), (22,1), (23,1), (24,1), (27,1), (34,11)
0.5	7	22	14.5	(2,1), (9,2), (13,1), (14,1), (15,2), (16,1), (17,2), (18,1), (19,1), (20,1), (21,1), (22,1), (23,1), (24,1)

optimal results of using SA in larger fields 5 m × 4 m, 5 m × 5 m and 6 m × 6 m with weight comparison.

In the experimental environment, the drift of the signal is obvious so that we use the median filter to remove the signal drift and take the example of − 14 dbm and power ranking 3. The results before and after applying the median filter are shown in Fig. 10. One can see that the number of power ranking 3 is reduced by 6 after using the median filter. In order to produce the best RSS profiles, we apply the median filter to reduce noise interferences including multipath effect and signal drift, respectively. Then, we measure 100 times at each position to see how many times it will be judged correctly. The measurement results are shown in Fig. 11.

Accordingly, we can know that the correct rate of each location. Fig. 12 represents the average error calculated for each position. The average error is defined as follows:

Error rate = 1 − correct rate.

Average error rate = correct rate × error rate of correct rate (0) + error rate (the proportion of the error rate × error value).

In addition to the first field, we also tested the second field, the third field and the fourth field. The size of each field is listed in the first column of Table 11. Compared with [14], the proposed method has better results in the lowest average errors, highest

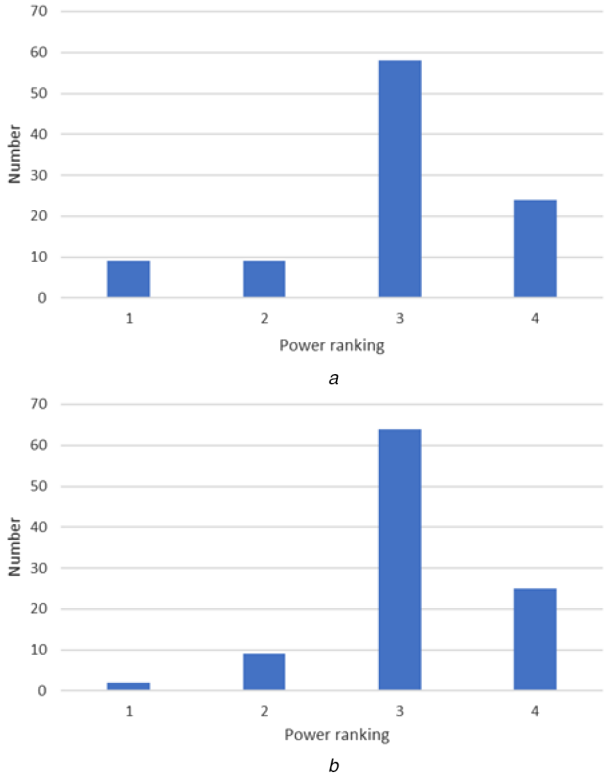

Fig. 10 *Results of using the median filter to remove the signal drift in the example of − 14 dbm and power ranking 3*
(a) Results before applying the median filter, ***(b)*** Results after applying the median filter

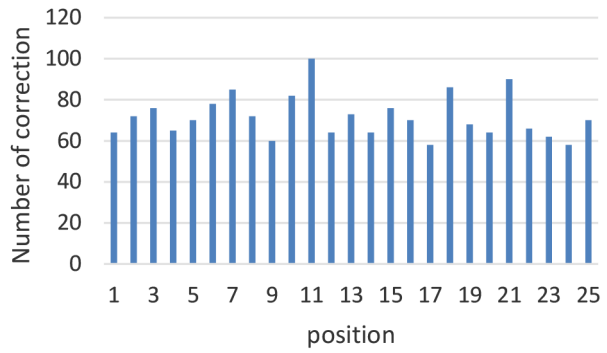

Fig. 11 *Number of corrections in testing 100 times*

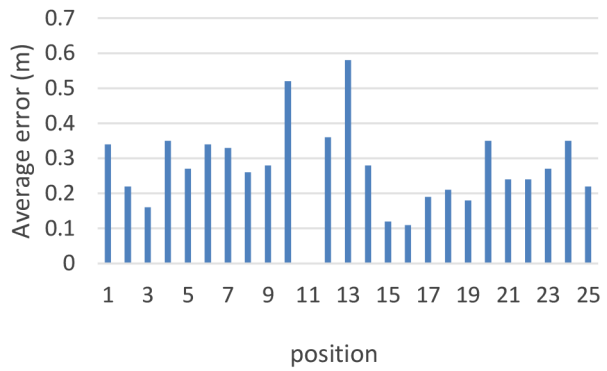

Fig. 12 *Average error (m) in each position*

average errors and average errors. The comparison is shown in Table 11.

4.3.2 Optimisation-based model phase II: In the second model, as shown in Figs. 13 and 14, the power options of 2, 3, 5 were tested in the field size of 5 m × 5 m and 7 m × 7 m by limiting the

Table 11 Comparison with [14]

Method		Lowest average errors, m	Highest average errors, m	Average errors, m
[14] (size 50 m × 50 m, ceiling height 3 m)		1.58	2.45	2.015
the proposed method	the first field (size 5 m × 5 m, ceiling height 2.4 m)	0	0.58	0.2708
	the second field (size 10 m × 10 m, ceiling height 2.4 m)	0.14	0.67	0.3802
	the third field (size 15 m × 15 m, ceiling height 3 m)	0.19	0.71	0.4263
	the fourth field (size 50 m × 50 m, ceiling height 3 m)	0.92	2.19	1.2725

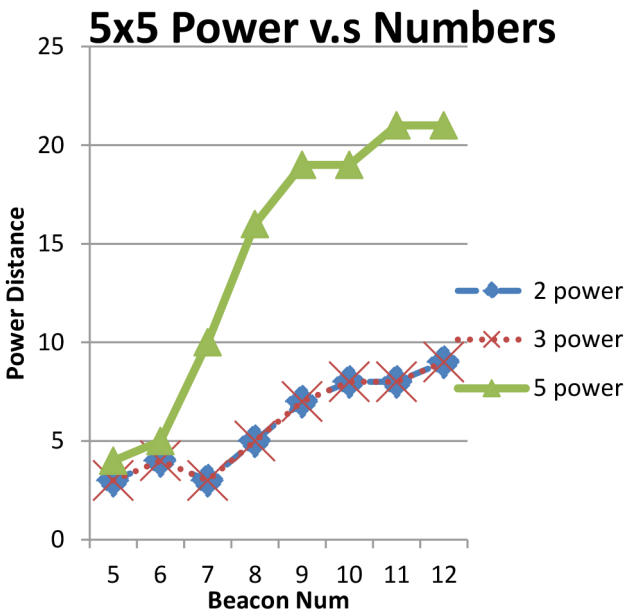

Fig. 13 *Relationship between power distance and number of beacon in 5 m × 5 m field*

number of beacons. From these two figures, it can be observed that the power distance is larger when the power is larger.

5 Conclusion

In this paper, the test field is divided into the grids and the proposed SPR in positioning enhances the discrimination. Moreover, an optimisation-based model for the deployment problem of beacons in indoor positioning is proposed on the basis of the two requirements, full coverage and full discrimination. The proposed model is novel and useful due to the feature of linear programming. Finally, the algorithm of SA is applied to obtain optimal results. Experimental results verify the performance and show that most positioning errors are <0.3 m and the average error is 0.2708 m in small size field 5 m×5 m.

6 Acknowledgments

This work was financially supported by the 'Intelligence Recognition Industry Service Research Center (IR-IS Research Center)' from The Featured Areas Research Center Program within the framework of the Higher Education Sprout Project by the Ministry of Education (MOE) in Taiwan.

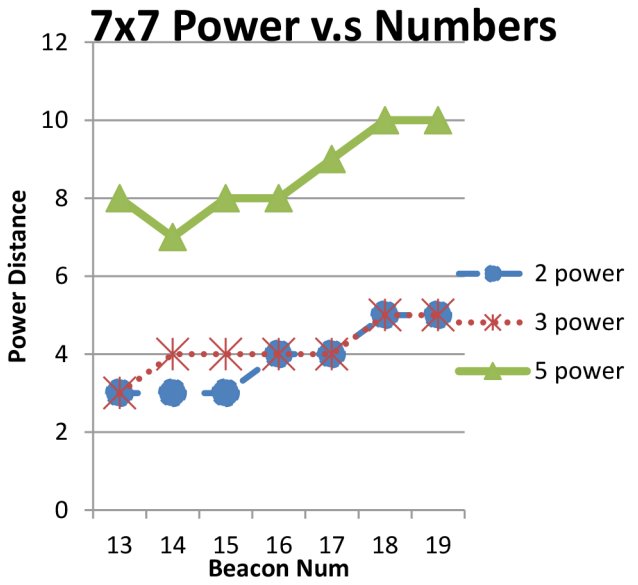

Fig. 14 *Relationship between power distance and number of beacon in 7 m × 7 m field*

7 References

[1] Adalja Disha, M.: 'A comparative analysis on indoor positioning techniques and systems', *Int. J. Eng. Res. Appl. (IJERA)*, 2013, **3**, (2), pp. 1790–1796

[2] Doiphode, S., Bakal, J.W., Gedam, M.: 'Survey of indoor positioning measurements, methods and techniques', *Int. J. Comput. Appl.*, 2016, **140**, (7), pp. 1–4

[3] Dwiyasa, F., Lim, M.-H.: 'A survey of problems and approaches in wireless-based indoor positioning'. Int. Conf. on Indoor Positioning and Indoor Navigation (IPIN), Alcala de Henares, Spain, 4–7 October 2016

[4] He, Z., Cui, B., Zhou, W., *et al.*: 'A proposal of interaction system between visitor and collection in museum hall by iBeacon'. Tenth Int. Conf. Computer Science & Education (ICCSE), 2015, Cambridge, UK., July 2015, pp. 427–430

[5] Zuo, Z., Liu, L., Zhang, L., *et al.*: 'Indoor positioning based on bluetooth low-energy beacons adopting graph optimization', *Sensors*, 2018, **18**, p. 3736, doi: 10.3390/s18113736

[6] Tolza, X., Acco, P., Fourniols, J.-Y., *et al.*: 'Optimal uncalibrated RSS indoor positioning and optimal reference node placement using cramér-rao lower bound', *J. Sens.*, 2019, **2019**, pp. 1–12, Article ID 5494901, https://doi.org/10.1155/2019/5494901

[7] Martin, P., Ho, B.J., Grupen, N., *et al.*: 'An iBeacon primer for indoor localization: demo abstract'. Proc. First ACM Conf. on Embedded Systems for Energy-Efficient Buildings, BuildSys '14; ACM, New York, NY, USA, 2014, pp. 190–191

[8] Boukerche, A., Oliveira, H.A.B.F., Nakamura, E.F., *et al.*: 'Localization systems for wireless sensor networks', *IEEE Wirel. Commun.*, 2007, **14**, pp. 6–12

[9] Mahiddin, N.A., Safie, N., Nadia, E., *et al.*: 'Indoor position detection using WiFi and trilateration technique'. Proc. Int. Conf. on Informatics and Applications (ICIA2012), Kuala Terengganu, Malaysia, 2–5 June 2012, pp. 362–366

[10] Dahlgren, E., Mahmood, H.: 'Evaluation of Indoor Positioning Based on Bluetooth Smart technology', Master's Thesis, Chalmers University of Technology, Gothenburg, Sweden, 2014

[11] Chen, Z., Zou, H., Jiang, H., *et al.*: 'Fusion of WiFi: smartphone sensors and landmarks using the kalman filter for indoor localization', *Sensors*, 2015, **15**, pp. 715–732

[12] Chen, Z., Zhu, Q., Soh, Y.C.: 'Smartphone inertial sensor-based indoor localization and tracking with iBeacon corrections', *IEEE Trans. Ind. Inform.*, 2016, **12**, pp. 1540–1549

[13] Zhuang, Y., Yang, J., Li, Y., *et al.*: 'Smartphone-based indoor localization with bluetooth low energy beacons', *Sensors*, 2016, **16**, p. 596, doi: 10.3390/s16050596

[14] Subedi, S., Kwon, G.-R., Shin, S., *et al.*: 'Beacon based indoor positioning system using weighted centroid localization approach'. 2016 Eighth Int. Conf. on Ubiquitous and Future Networks (ICUFN2016), Vienna Austria, 5–8 July 2016

[15] Danis, F.S., Cemgil, A.T.: 'Model-based localization and tracking using bluetooth low-energy beacons', *Sensors*, 2017, **17**, p. 2484, doi: 10.3390/s17112484

[16] Liu, R., Yuen, C., Do, T., *et al.*: 'Fusing similarity-based sequence and dead reckoning for indoor positioning without training', *IEEE Sens. J.*, 2017, **17**, (13), pp. 4197–4207

[17] Yassin, A., Nasser, Y., Awad, M., *et al.* 'Recent advances in indoor localization: A survey on theoretical approaches and applications', *IEEE Commun. Surv. Tutorials*, 2017, **19**, (2), pp. 1327–1346

[18] Tekinay, S.: 'Wireless geolocation systems and services', *IEEE Commun. Mag.*, 1998, **36**, (4), pp. 28–29

[19] Krumm, J., Harris, S., Meyers, B., *et al.*: 'Multi-camera multi-person tracking for easy living'. Proc. of IEEE Int. Workshop on Visual Surveillance, Washington, DC, July 2000, pp. 3–10

[20] Gigl, T., Janssen, G.J.M., Dizdarevic, V., *et al.*: 'Analysis of a UWB indoor positioning system based on received signal strength'. WPNC '07, Fourth Workshop on Positioning, Navigation and Communication, Hannover, Germany, 2007, pp. 97–101

[21] Azuma, R.: 'Tracking requirements for augmented reality', *Communications of ACM*, 1993, **36**, (7), pp. 50–51

[22] Maddumabandara, A., Leung, H., Liu, M.: 'Experimental evaluation of indoor localization using wireless sensor networks', *IEEE Sens. J.*, 2015, **15**, (9), pp. 5228–5237

[23] De Angelis, G., Pasku, V., De Angelis, A., *et al.*: 'An indoor AC magnetic positioning system', *IEEE Trans. Instrum. Meas.*, 2015, **64**, (5), pp. 1267–1275

[24] Chen, Y., Lymberopoulos, D., Liu, J., *et al.*: 'Indoor localization using FM signals', *IEEE Trans. Mob. Comput.*, 2013, **12**, (8), pp. 1502–1517

[25] Fard, H.K., Chen, Y., Son, K.K.: 'Indoor positioning of Mobile devices with Agile iBeacon placement'. 2015 IEEE 28th Canadian Conf. on Electrical and Computer Engineering (CCECE), Halifax, NS, Canada, May 2015

[26] Varshney, V., Goel, R.K., Abdul Qadeer, M.: 'Indoor positioning system using Wi-Fi & bluetooth low energy technology'. Thirteenth Int. Conf. on Wireless and Optical Communications Networks (WOCN), Hyderabad, India, 2016

[27] Mackensen, E., Lai, M., Wendt, T.M.: 'Bluetooth low energy (BLE) based wireless sensors'. 2012 IEEE Sensors, Taipei, Taiwan, October 2012, p. 12

[28] Raza, S., Misra, P., He, Z., *et al.*: 'Bluetooth smart: an Enabling technology for the internet of things'. 2015 IEEE 11th Wireless and Mobile Computing, Networking and Communications (WiMob), Abu Dhabi, United Arab Emirates, October 2015, pp. 155–162

[29] Köhne, M., Sieck, J.: 'Location-based services with iBeacon technology'. 2014 2nd Int. Conf. on Artificial Intelligence, Modelling & Simulation (AIMS), Madrid, Spain, November 2014

[30] Granville, V., Krivanek, M., Rasson, J.-P.: 'Simulated annealing: A proof of convergence', *IEEE Trans. Pattern Anal. Mach. Intell.*, 1994, **16**, (6), pp. 652–656